Overexpression of adenylate cyclase-associated protein 1 may predict brain metastasis in non-small cell lung cancer

SHUAN-SHUAN XIE, MIN TAN, HAI-YAN LIN, LEI XU, CHANG-XING SHEN, QING YUAN, XIAO-LIAN SONG and CHANG-HUI WANG

Department of Respiratory Medicine, Shanghai Tenth People's Hospital, Tongji University, Shanghai 200072, P.R. China

Received August 7, 2014; Accepted October 9, 2014

DOI: 10.3892/or.2014.3577

Abstract. This study was designed to establish a biomarker risk model for predicting brain metastasis (BM) in non-small cell lung cancer (NSCLC). The model comprises 120 cases of NSCLC that were treated and followed up for 4 years. The patients were divided into the BM (n=50) and non-BM (other visceral metastasis and those without recurrence) (n=70) groups. Immunohistochemical and western blot analyses were performed in metastatic tissues of NSCLC. Multivariate regression analysis was performed to correlate the immunoreactive cyclase-associated protein 1 (CAP1) signal with BM. Survival analyses were performed by using the Kaplan-Meier method. CAP1 protein content and immunoreactivity were significantly increased in BM specimens compared to other-metastatic specimens. The survival analysis revealed that CAP1 overexpression was significantly associated with survival (P<0.05). The ROC test suggested that the area under the curve was 73.33% (P<0.001; 95% CI, 63.5-83.2%). When P=0.466, the sensitivity and specificity reached 79.5 and 67.1%, respectively. These findings suggested that CAP1 is involved in the BM of NSCLC, and that elevated levels of CAP1 expression may indicate a poor prognosis for patients with BM. The CAP1 molecular model may be useful in the prediction of the risk of BM in NSCLC.

Introduction

Lung cancer is the leading cause of cancer-related mortality in men and women, resulting in ~221,130 new cases and 156,940 deaths in the United States, and ~1.3 million deaths per year worldwide. Non-small cell lung cancer (NSCLC) accounts for ~85% of all lung cancers, and the 5-year survival of patients with metastatic NSCLC is <10% (1-3).

Brain metastasis (BM) is a frequent occurrence in NSCLC patients. The BM incidence ranges from 17 to 54% as the first site of recurrence in 15-40% of cases (4-6), and this risk is >50% in patients with small cell lung cancer (SCLC). Although most patients achieved some palliation, surgery, and chemotherapy >50% of them succumbed due to intracranial progression, and the median survival was 3-6 months (7-11). BM is therefore a common and devastating event in NSCLC patients with a poor outcome regardless of the treatment administered.

Biomarkers are critical to early diagnosis and prediction and monitoring of progressive lesions. BM is the main cause of treatment failure. If BM can be predicted at an early stage, then effective prevention may be initiated and result in an improvement in survival. Few studies have focused on the correlation between biomarkers and BM, while none have been routinely used clinically. It is, therefore, crucial to identify more reliable and feasible novel biomarkers for BM of NSCLC. The present study assessed the diagnostic and prognostic value of cyclase-associated protein 1 (CAP1) to predict the risk of BM in NSCLC in order to screen patients at high risk of BM for early intervention.

Patients and methods

Ethical considerations. The study was reviewed and approved by the Institutional Ethics Committee of the Shanghai Tenth People's Hospital of Tongji University and was conducted in compliance with the Helsinki Declaration. Written informed consent was obtained from all subjects.

Patients selection. Patients with NSCLC were considered eligible if they had stable disease or better (i.e., complete or partial response) after potentially curative therapy, defined as high-dose thoracic radiation therapy (RT, >30 Gy) or surgery. Radiation was administered with or without neoadjuvant, adjuvant, or concurrent chemotherapy. Pre- or post-operative RT and/or chemotherapy were acceptable. Therapy had to have been completed within 10 weeks of study entry. Patients were restaged with computed tomography (CT) scan of the chest and abdomen and magnetic resonance imaging (MRI) of the brain and bone within 3 weeks of study entry. Contrast-enhanced CT of the brain and bone was considered acceptable if MRI

Correspondence to: Professor Xiao-Lian Song or Professor Chang-Hui Wang, Department of Respiratory Medicine, Shanghai Tenth People's Hospital, Tongji University, 301 Yanchang Middle Road, Shanghai 200072, P.R. China
E-mail: song-xiao-lian@hotmail.com
E-mail: wang-chang-hui@hotmail.com

Key words: lung cancer, brain metastasis, biomarker

was contraindicated and if performance for pretreatment assessment was required for follow-up imaging.

Patients were not required to have evidence of progressive intrathoracic disease, brain metastases, bone metastases, or visceral metastases. Any acute or subacute grade ≥3 toxicities from previous therapy were required to have decreased to grade ≤2 at the time of study entry.

Follow-up and database construction. The patients were stratified by age (≤65 and >65 years), Zubrod performance status (0 and >0), histology (adenocarcinoma and non-adenocarcinoma), T-stage (T1, T2, T3 and T4), N-stage (N0, N1, N2 and N3), tumor size (≤3 and >3 cm), and therapy (surgery or none). Samples were collected from June, 2008 to December, 2009 at Shanghai Tenth People's Hospital, and were followed up until December 2013.

The patients were followed up regularly by designated staff, who collected all the information in a central database. The patients were followed 3-4 times a year in the first 2 years, and once every six months in the following 2 years. The last follow-up visit was on December, 2013. The basic demographic and clinical characteristics of initial and outcome patient variables, including age, gender, Zubrod performance status, histopathology, stage, tumor size and prior chemotherapy/RT/surgery, are shown in Table I.

Pulmonary metastasis analysis and biopsy specimen collection. Specimens of 39 brain metastasis, and 70 non-metastasis patients who underwent surgical resection for neoplastic, at the Shanghai Tenth People's Hospital (Shanghai, China), were collected after follow up between 2009 and 2013. Cancer types and stages were determined based on results from laboratory tests, X-rays, as well as CT, brain and MRI scans. Biopsy specimens were collected at surgery, snap-frozen in liquid nitrogen and stored at -80˚C until analysis.

H&E and immunohistochemical (IHC) SP assay. H&E sections were examined under a microscope to identify and mark the cancer nests. The formalin-fixed and paraffin-embedded (FFPE) sections were dewaxed in xylene and rehydrated in graded ethanol. Endogenous peroxidase activity was blocked by soaking in 0.3% hydrogen peroxide. The sections were then processed in 10 mmol/l citrate buffer (pH 6.0) and heated to 121˚C in an autoclave for 20 min to retrieve the antigen. After rinsing in phosphate-buffered saline (PBS) (pH 7.2), 10% goat serum was applied for 1 h at room temperature to block any non-specific reactions. The sections were then incubated overnight at 4˚C with anti-CAP1 (diluted at 1:500; mouse anti-human monoclonal antibodies against CAP1 was provided by Dr Zhou, University of Pennsylvania School of Medicine (Philadelphia, PA, USA). All the slides were processed using the peroxidase-antiperoxidase method (Dako, Hamburg, Germany). After rinsing with PBS, the peroxidase reaction was visualized by incubating the sections with diaminobenzidine tetrahydrochloride in 0.05 mol/l Tris buffer (pH 7.6) containing 0.03% H_2O_2. After rinsing in water, the sections were counterstained with hematoxylin, dehydrated and coverslipped. Stained sections were observed under a microscope. At least 10 high-power fields were randomly chosen, and ≥400 cells/field were counted.

Staining results were independently assessed by two pathologists, who were blind to the specimens. The immunoreactive intensity in the test tissue specimens was graded by the difference against the intensity in endothelial cells in the positive control group: 0, negative; 1 (weak), weaker than epithelial cells; 2 (moderate), the same as epithelial cells; 3 (strong), stronger than epithelial cells. A staining score of 2 or 3 was considered CAP1-positive.

Western blot analysis. Tissue samples were immediately homogenized in buffer containing 1 M Tris-HCl (pH 7.5), 1% Triton X-100, 1% NP-40 (Nonidet P-40), 10% sodium dodecyl sulfate (SDS), 0.5% sodium deoxycholate, 0.5 M EDTA, 10 mg/ml leupeptin, 10 mg/ml aprotinin and 1 mM PMSF. The samples were centrifuged at 10,000 x g for 30 min to collect the supernatant. Proteins were mixed with loading and DTT (4:5:1) twice, boiled in water for 5-10 min and cooled in ice. Protein concentrations were determined using a Bio-Rad protein assay (Bio-Rad, Hercules, CA, USA), and following total protein quantification, the lysates were loaded onto 10% polyacrylamide-SDS gels, separated by electrophoresis and blotted onto NC membrane blots using a semi-dry transfer system. The blots were incubated with a mouse anti-human CAP1 antibody and a mouse anti-human actin antibody (both from Sigma, St. Louis, MO, USA) at 4˚C overnight. After washing, the blots were incubated with horseradish peroxidase-conjugated secondary antibodies at room temperature for 45 min. The immunoreactive signals for CAP1 and actin were visualized using the ECL system from GE Healthcare UK, Ltd. (Little Chalfont, Buckinghamshire, UK) and subjected to densitometric analyses using ImageJ software (National Institutes of Health, Bethesda, MD, USA). Relative levels of CAP1 (after adjustment against actin) were determined based on the densitometric data.

Quantitative PCR. Total RNA was isolated from biopsy specimens using an RNA extraction kit from Isogen (Nippon Gene Co., Ltd., Toyama, Japan). RNA samples were treated with DNase I (Promega Corp., Madison, WI, USA) to remove genomic DNA. First-strand cDNAs were synthesized using a commercial First-Strand cDNA Synthesis kit as per the manufacturer's instructions. PCR amplifications of the test gene *CAP1* and the reference gene glyceraldehyde-3-phosphate dehydrogenase (*GAPDH*) were performed using the primers, forward: 5'-ACT CGC TGC TTG CTG GTC-3' and reverse: 5'-ATG GGT GCC AAC AAA TCG-3', designed based on the human CAP1 mRNA sequence (GenBank accession no. BT007152) and the primers, forward: 5'-GAA GGT GAA GGT CGG AGTC-3' and reverse: 5'-CCC GAA TCA CAT TCT CCA AGA A-3', designed based on the human GAPDH cDNA sequence (GenBank access no. X01677). The reactions were carried out with the SYBR-Green PCR Core Reagents kit (Perkin-Elmer Applied Biosystems, Foster City, CA, USA). The PCR amplification parameters were: 50˚C for 2 min (one cycle), 95˚C for 10 min (one cycle), 95˚C for 15 sec and 60˚C for 1 min (40 cycles). The emission intensity of the SYBR-Green fluorescence was measured as real-time using the ABI PRISM 7700 Sequence Detector from Perkin-Elmer Applied Biosystems. Relative quantification of CAP1 mRNA abundance was performed using the DataAssist software (Life Technologies, Grand Island, NY, USA).

Table I. The basic demographic and clinical characteristics of initial and outcome patient variables.

Variables	Initial patient characteristics: 120 evaluable patients			Outcome patient characteristic after 4-year follow-up	
	Patients (n)	Percentage (%)	Brain metastasis (n=50), n (%)	Non-brain metastasis (n=70), n (%)	P-value
Gender					
Male	77	64.17	32 (64.00)	45 (64.30)	
Female	43	35.83	18 (36.00)	25 (35.70)	0.974
Age (years)					
≤65	80	66.67	31 (62.00)	32 (45.70)	
>65	40	33.33	19 (38.00)	38 (54.30)	0.078
Zubrod performance status					NA[a]
0	56	46.67	26	30	
1	54	45.0	17	37	
2	6	5	4	2	
3	1	0.83	1	0	
Unknown	3	2.5	2	1	
0	56	46.67	26 (52.00)	30 (42.90)	
>0	64	53.33	24 (48.00)	40 (57.10)	0.322
Histopathology					NA[a]
Adenocarcinoma	49	40.83	24	25	
Squamous cell carcinoma	25	20.83	10	15	
Large-cell undifferentiated	15	12.5	6	9	
Combined/mixed	0	0	0	0	
Non-small cell carcinoma, NOS	29	24.17	9	20	
Other	2	1.7	1	1	
Adenocarcinoma	49	40.83	24 (48.00)	25 (35.70)	
Non-adenocarcinoma	71	59.17	26 (52.00)	45 (64.30)	0.177
T-stage					NA[a]
T1	25	20.83	10	15	
T2	35	29.17	11	24	
T3	34	28.3	19	15	
T4	26	21.7	10	16	
N-stage					NA[a]
N0	51	42.5	17	34	
N1	14	11.7	9	5	
N2	43	35.8	18	25	
N3	12	10	6	7	
Tumor size (T) (cm)					
≤3	66	55.0	24 (48.00)	42 (60.00)	
>3	54	45.0	26 (52.00)	28 (40.00)	0.193
Prior chemotherapy/RT					NA[a]
Chemotherapy/RT	106	88.3	44	62	
Chemotherapy alone	4	3.3	3	1	
RT alone	10	8.3	3	7	
Prior surgery					
No	64	53.3	30 (60.00)	33 (47.10)	
Yes	56	46.7	20 (40.00)	37 (52.90)	0.164
Entire prior therapy regimen					NA[a]
RT and chemotherapy	58	48.3	28	30	
RT only	6	5	4	2	
Surgery and chemotherapy	2	1.7	1	1	
Surgery and RT	4	3.3	2	2	
Surgery, RT and chemotherapy	50	41.7	15	35	

[a]Insufficient cell counts. Total no. of patients, 120. NOS, not otherwise specified; RT, radiation therapy; NA, not applicable; all, with an χ^2 test.

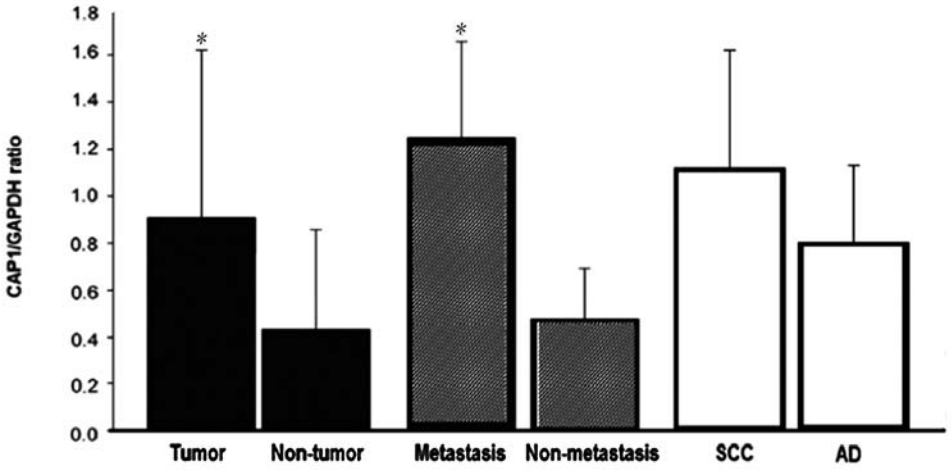

Figure 1. Relative cyclase-associated protein 1 (CAP1) mRNA levels [CAP1/glyceraldehyde-3-phosphate dehydrogenase (GAPDH) mRNA ratio] in non-neoplastic lung tissue and lung tumors of different stage and histological type. *P<0.05, comparison made within the same type of bar.

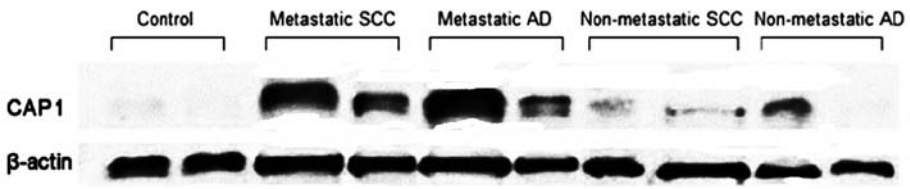

Figure 2. A representative western blot analysis showing cyclase-associated protein 1 (CAP1) and β-actin bands in indicated biopsy specimens (two representative samples from each of the patient groups).

Statistical analysis. Statistical analysis was performed using SPSS version 20.0. Categorical data expressed as a percentage were analyzed using the χ^2 test. Multivariate Cox proportional hazard and logistic regression analysis models were utilized to determine the correlations between CAP1 expression and various clinicopathological variables. The models were also examined by the receiver operating characteristics (ROC) analysis. For analysis of survival data, Kaplan-Meier curves were constructed. Differences were considered significant when P<0.05. The results are expressed as the mean ± standard error (SE).

Results

Findings of previous and recent studies. In a recent study, Tan *et al* (12) demonstrated that the relative CAP1 mRNA abundance, expressed as the CAP1/GAPDH ratio, was significantly higher in neoplastic tissues than in control specimens (P=0.028), and in metastatic than in non-metastatic lung cancer specimens (P=0.016). A comparison performed between histological types showed that squamous cell carcinoma (SCC) specimens had slightly higher CAP1 mRNA abundance than adenocarcinoma (AD) specimens, although the difference did not reach a statistically significant level (P=0.227) (Fig. 1).

In addition, CAP1 protein levels in biopsy specimens were determined by western blot analysis. The relative CAP1 protein level was significantly elevated in lung cancer patients (0.7527±0.2767) as compared to non-neoplastic control subjects (0.3476±0.1713, P=0.002). It was also significantly elevated in metastatic lung tumors (0.8941±0.1442) as compared to non-metastatic lung tumors (0.4701±0.2647, P=0.002). The CAP1 protein level was slightly higher in SCC than in AD specimens (0.7440±0.2911 vs. 0.7601±0.2757, P=0.891), although the difference was not significant (P>0.05) (Fig. 2).

The results of western blot analysis were even more apparent in brain metastasis of SCC and AD as compared to other metastatic groups such as the bone- and visceral-metastatic groups (Fig. 3). Therefore, experiments were conducted to elucidate this phenomenon.

Demographic characteristics. Patient samples were collected from June, 2008 to December, 2009, and patients were followed up until December 2013. The patients were followed up 3-4 times a year in the first 2 years, and once every six months in the following 2 years. Of the 156 patients included in this study, 17 SCLC patients were ineligible, 11 patients withdrew consent and the 128 patients remaining were followed up for 4-years. Eight of the 128 patients were lost to follow-up, while data from 120 cases of NSCLC patients were analyzed. After the 4-year follow up, we analyzed outcome patient characteristics including 50 cases with brain metastasis, and 70 cases without brain metastasis (Fig. 4).

All the patients had complete resection of the tumor and were staged according to UICC 1999. The patients included 77 males and 43 females, aged 63.24 (range, 30-85) years. Pathological examination showed 49 cases of adenocarcinoma, and 71 cases of non-adenocarcinoma. After the 4-year follow up, the 50 cases of brain metastasis were designated as

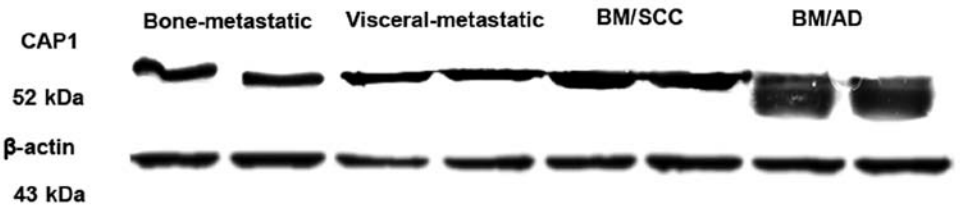

Figure 3. A representative western blot analysis showing cyclase-associated protein 1 (CAP1) and β-actin bands in indicated metastatic biopsy specimens (two representative samples from each of the patient groups). BM, brain metastasis; AD, adenocarcinoma; SCC, squamous cell carcinoma.

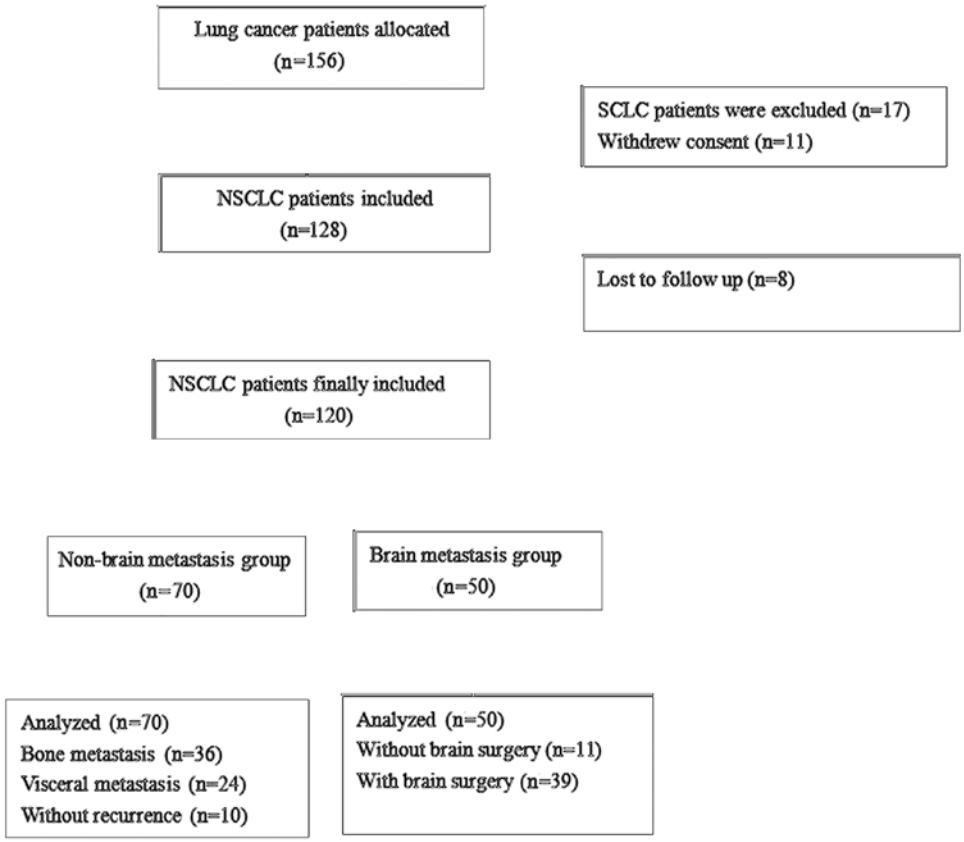

Figure 4. Flow diagram of study identification. NSCLC, non-small-cell lung cancer; SCLC, small cell lung cancer.

Table II. Correlation between immunoreactive CAP1 signals and brain metastasis.

Biomarkers	Brain metastasis, n (%)	Non-brain metastasis, n (%)	P-value
CAP1 +	31 (79.5)	23 (32.9)	<0.01
CAP1 -	8 (20.5)	47 (67.1)	

CAP1, cyclase-associated protein 1.

the brain metastasis group. The remaining 70 cases with bone, visceral or without metastasis were defined as the non-brain metastasis group. No statistically significant difference was found between the brain metastasis and non-brain metastasis groups in terms of clinical and pathological factors (Table I).

Correlation between immunoreactive CAP1 signals and cancer metastasis. H&E sections were initially examined under a microscope to identify and mark the cancer nest brain specimens (Fig. 5). CAP1 associated with brain metastasis was assessed by immunohistochemical analysis. The χ^2 test showed that CAP1 was associated with brain metastasis (P<0.01) (Table II). Immunoreactive CAP1 was detected in the cytoplasm of cancer cells in all 39 brain metastasis samples. It was found that CAP1 immunoreactivity was highly expressed in lung cancer with brain metastasis but was weakly expressed in lung cancer tissues without brain metastasis. In addition, when CAP1 was highly expressed in lung tissues, it was also highly expressed in brain tissues (Fig. 6).

The 39 brain samples were classified into a CAP1-negative group, where the tumor staining score was 0 or 1, and a CAP1-positive group, where the tumor staining score was 2 or 3. The relationship between clinicopathological background and IHC of CAP1 expression is shown in Table III. Increased

Table III. CAP1 expression and clinicopathological characteristics in 39 brain specimens.

Characteristics	Total, n (%)	CAP1-negative	CAP1-positive, n	P-value
Gender				
Male	25 (64.1)	10	15	0.729
Female	14 (35.9)	4	10	
Age (years)				
≤65	24 (61.5)	10	14	0.274
>65	15 (38.5)	4	11	
Histopathology				
Adenocarcinoma	18 (46.2)	5	13	0.261
Non-adenocarcinoma	21 (53.8)	9	12	
Tumor size (T) (cm)				
≤3	20 (51.3)	12	8	0.02
>3	19 (48.7)	2	17	
Adjuvant chemotherapy				
Yes	20 (51.3)	5	15	0.131
No	19 (48.7)	9	10	
Adjuvant radiation therapy				
Yes	17 (43.6)	6	11	0.607
No	22 (56.4)	8	14	

CAP1, cyclase-associated protein 1.

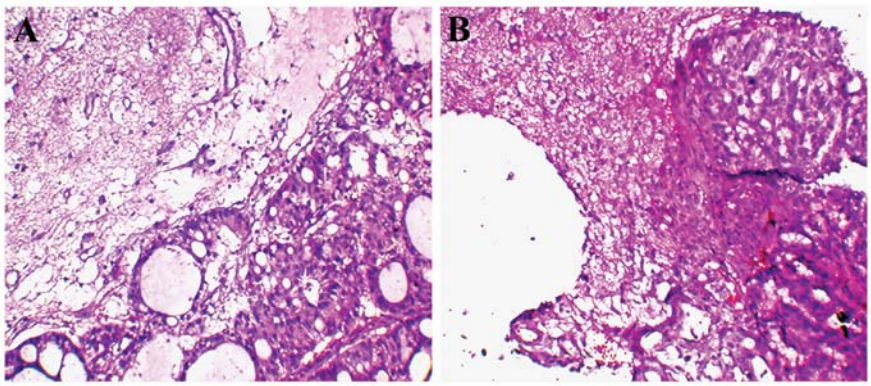

Figure 5. Hematoxylin and eosin (H&E) staining of histological tissues. H&E in brain metastasis of non-small cell lung cancer (NSCLC) patients. Brain biopsy specimens showing (A) squamous cell carcinoma (SCC) and (B) adenocarcinoma (AD) cancer nests.

expression of CAP1 exhibited a significant correlation with tumor sizes (P=0.02), while there were no correlations between CAP1 and age, gender, histopathology, adjuvant chemotherapy and adjuvant RT. In addition, a multivariate Cox proportional hazard model was constructed comparing factors including age, grade, tumor size, histopathology, adjuvant chemotherapy, adjuvant RT and CAP1 expression. CAP1 expression and tumor size were independent prognostic factors in NSCLC patients with brain metastasis (P<0.01 and P=0.047, respectively) (Table IV).

Establishment of the prediction model of brain metastasis. The ROC analysis (Fig. 7) suggested that the area under the curve was 73.33% (P<0.01; 95% CI, 63.5-83.2%). When P=0.466, the sensitivity and specificity reached 79.5 and 67.1%, respectively. Thus, P≥0.466 can be used as the screening indicator in this model to identify patients at high risk of brain metastasis in NSCLC.

CAP1 overexpression is associated with poor prognosis. The Kaplan-Meier survival analysis revealed the poor outcome of patients in the high-level CAP1-expression group (Fig. 8B and C), and 5-year survival rates were 19 and 59% in the high- and low-level groups (P=0.030, log-rank test). In addition, although the time-adjusted incidence of brain metastasis did not significantly differ between the high and low expression of CAP1, the low CAP1 appeared to delay the onset of late brain metastasis (P=0.0404) (Fig. 8A). These results

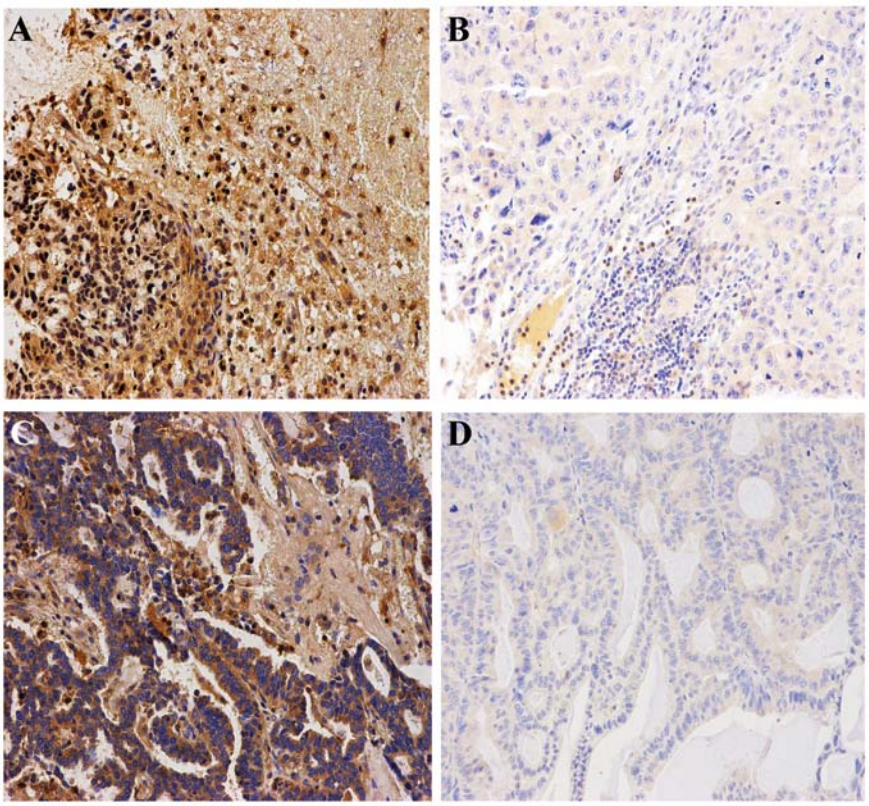

Figure 6. Representative sections of pathological brain specimens following immunohistochemical staining. (A) Brain metastases from squamous cell carcinoma (SCC) showing a high percentage of cyclase-associated protein 1 (CAP1)-positive cells. (B) Brain metastases from SCC showing a low percentage of CAP1-positive cells. (C) Brain metastases from adenocarcinoma (AD) showing a high percentage of CAP1-positive cells. (D) Brain metastases from AD showing a low percentage of CAP1-positive cells.

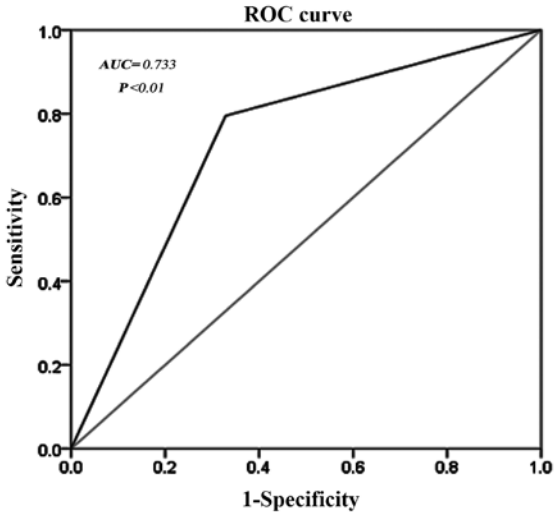

Figure 7. ROC curve of the biomarker model for predicting brain metastasis in non-small cell lung cancer.

indicated that the expression level of CAP1 is associated with tumor size, which can be associated with shorter survival of NSCLC patients with brain metastasis.

Discussion

Between 25 and 40% of NSCLC patients reportedly develop BM during the course of their disease. The majority of BM (80%) generally occur in the cerebral hemispheres, 15% in the cerebellum, and 5% in the brainstem (13). BM patients frequently require therapeutic intervention in the form of RT, surgery and chemotherapy, which may considerably add to the cost of their end-of-life care. In addition, BM from NSCLC is associated with numerous negative effects on the patient quality of life and survival. At the present time, there are no proven treatments for cognitive impairment following brain cancer and no known effective preventive strategies.

Adenylate CAP1 is an actin monomer-binding protein coded by the *CAP1* gene (14), which was originally cloned from budding yeast and is located downstream of the *ras* gene (15). Human homology of CAP1 was identified in the early 1990s (16). Both mammal and yeast CAPs interact with actin (17) and play a role in actin turnover (18). Given the critical role for actin filament reorganization in cell migration and the regulatory role for CAP1 in actin filament reorganization (19,20), it may be hypothesized that CAP1 is associated with tumor metastasis. However, only a few studies have reported CAPs in mammalian cells and human cancer (21). The involvement of CAP1 in the aggressive behavior of pancreatic cancer cells has been reported (21). In this study, the relationship between the expression of CAP1 and the migration of BM was identified.

To evaluate the association of CAP1 and BM, we first assessed *CAP1* gene expression at the protein level in brain metastases of SCC and AD as compared to other metastatic groups, such as bone- and visceral-metastatic subjects by

Table IV. Contribution of various potential prognostic factors to survival by Cox regression analysis in 39 brain specimens.

Values	B	SE	Wald	P-value	Exp (B)	95% CI for Exp (B) lower-upper
Gender	0.386	0.302	1.486	0.223	1.445	0.800-2.611
Age	0.045	0.360	0.016	0.900	1.046	0.516-2.120
Histopathology	10.285	0.332	0.739	0.390	1.330	0.694-2.547
Tumor size (T) (cm)	1.126	0.568	3.936	0.047[a]	3.083	1.014-9.379
Adjuvant chemotherapy	1.120	0.735	2.323	0.127	3.065	0.726-12.944
Adjuvant radiation therapy	0.320	0.291	1.209	0.272	1.377	0.778-2.437
Expression of CAP1	1.757	0.400	19.238	<0.01[b]	5.793	2.642-12.700

[a]P<0.05, [b]P<0.01 was considered significant. Statistical analyses were performed by the Cox test. CAP1, cyclase-associated protein 1.

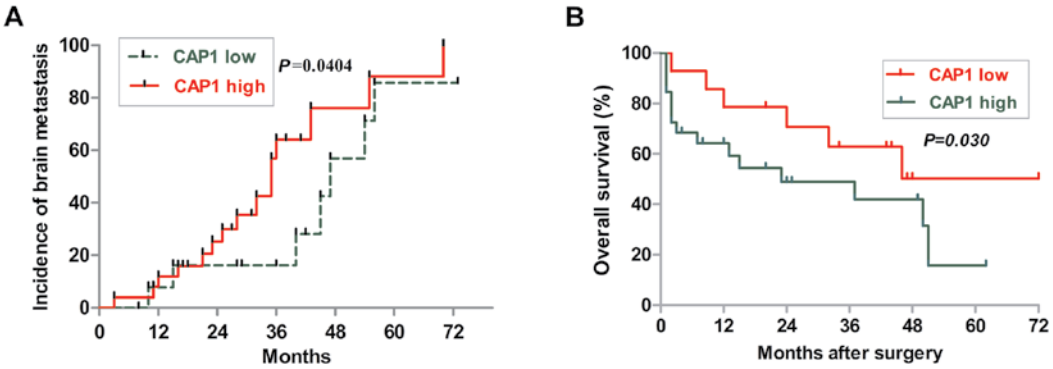

C

Number at risk

Months	0	12	24	36	48	60	72
CAP1 low	14	12	10	9	7	2	2
CAP1 high	25	14	10	7	5	1	0

Figure 8. (A) Time to brain metastasis analysis. Brain metastasis between high and low cyclase-associated protein 1 (CAP1)-positive rate. (B and C) Kaplan-Meier survival analysis. Overall survival (%) of patients with high and low CAP1-positive rate is shown by solid and dotted lines, respectively.

western blot analysis. The results clearly demonstrated that *CAP1* gene transcription was significantly elevated in brain metastasis patients and the elevation was more pronounced in AD lung cancer patients. To further evaluate the correlation between CAP1 expression and BM of NSCLC, 120 NSCLC patients were employed from June, 2008 to December, 2009, and were followed up until December, 2013. The results show that 50 patients developed BM while the 70 remaining patients developed other types of metastasis. In the present study, stronger immunoreactive CAP1 signals were detected in the perinuclear cytoplasm of BM in NSCLC in the biopsy specimens. The IHC analyses identified CAP1 overexpression in BM of NSCLC from the multivariate regression analysis. As a result, CAP1 was involved in BM. Furthermore, the result of the ROC curve demonstrated that CAP1 can establish the prediction model of BM. In addition, the ratio of BM, Kaplan-Meier survival and the high and low expression of CAP1 was analyzed.

To the best of our knowledge, this is the first study undertaken to evaluate the relationship between biomarker CAP1 and BM in NSCLC patients. Although the results are noteworthy, the limitations of this study should be acknowledged. This study was limited to a small number of NSCLC patients. In the future, a large-scale study focusing on different stages may be useful to assess the value of this prediction model.

In conclusion, the diagnostic and prognostic value of CAP1 was shown to be commonly overexpressed, and to predict the risk of BM in NSCLC in order to screen the patients at high risk of BM for early intervention. Taken together, our data have shown that CAP1 is a novel prognostic biomarker in BM of NSCLC.

Acknowledgements

This study was funded by the National Natural Science Foundation of China (nos. 81172229 and 81100018).

References

1. Siegel R, Ward E, Brawley O and Jemal A: Cancer statistics: the impact of eliminating socioeconomic and racial disparities on premature cancer deaths. CA Cancer J Clin 61: 212-236, 2011.
2. Walling J: Chemotherapy for advanced non-small-cell lung cancer. Respir Med 88: 649-657, 1994.
3. Govindan R, Page N, Morgensztern D, *et al*: Changing epidemiology of small-cell lung cancer in the United States over the last 30 years: analysis of the surveillance, epidemiologic, and end results database. J Clin Oncol 24: 4539-4544, 2006.
4. Strauss GM, Herndon JE, Sherman DD, *et al*: Neoadjuvant chemotherapy and radiotherapy followed by surgery in stage IIIA non-small-cell carcinoma of the lung: report of a Cancer and Leukemia Group B phase II study. J Clin Oncol 10: 1237-1244, 1992.
5. Albain KS, Rusch VW, Crowley JJ, *et al*: Concurrent cisplatin/etoposide plus chest radiotherapy followed by surgery for stages IIIA (N2) and IIIB non-small-cell lung cancer: mature results of Southwest Oncology Group phase II study 8805. J Clin Oncol 13: 1880-1892, 1995.
6. Andre F, Grunenwald D, Pujol JL, *et al*: Patterns of relapse of N2 non-small-cell lung carcinoma patients treated with preoperative chemotherapy: should prophylactic cranial irradiation be reconsidered? Cancer 91: 2394-2400, 2001.
7. Carmichael J, Crane JM, Bunn PA, *et al*: Results of therapeutic cranial irradiation in small cell lung cancer. Int J Radiat Oncol Biol Phys 14: 455-459, 1998.
8. Cox JD, Stanley K, Petrovich Z, *et al*: Cranial irradiation in cancer of the lung of all cell types. JAMA 245: 469-472, 1981.
9. Arriagada R, Le Chevalier T, Borie F, *et al*: Prophylactic cranial irradiation for patients with small-cell lung cancer in complete remission. J Natl Cancer Inst 87: 183-190, 1995.
10. Shaw EG, Su JQ, Eagan RT, *et al*: Prophylactic cranial irradiation in complete responders with small-cell lung cancer: analysis of the Mayo Clinic and North Central Cancer Treatment Group data bases. J Clin Oncol 12: 2327-2332, 1994.
11. Langer CJ and Mehta MP: Current management of brain metastases, with a focus on systemic options. J Clin Oncol 23: 6207-6219, 2005.
12. Tan M, Song X, Zhang G, *et al*: Overexpression of adenylate cyclase-associated protein 1 is associated with metastasis of lung cancer. Oncol Rep 30: 1639-1644, 2013.
13. Delattre JY, Krol G, Thaler HT and Posner JB: Distribution of brain metastases. Arch Neurol 45: 741-744, 1988.
14. Fedor-Chaiken M, Deschenes RJ and Broach JR: SRV2, a gene required for RAS activation of adenylate cyclase in yeast. Cell 61: 329-340, 1990.
15. Field J, Vojtek A, Ballester R, *et al*: Cloning and characterization of CAP, the *S. cerevisiae* gene encoding the 70 kd adenylyl cyclase-associated protein. Cell 61: 319-327, 1990.
16. Matviw H, Yu G and Young D: Identification of a human cDNA encoding a protein that is structurally and functionally related to the yeast adenylyl cyclase-associated CAP proteins. Mol Cell Biol 12: 5033-5040, 1992.
17. Freeman NL, Chen Z, Horenstein J, Weber A and Field J: An actin monomer binding activity localizes to the carboxyl-terminal half of the *Saccharomyces cerevisiae* cyclase-associated protein. J Biol Chem 270: 5680-5685, 1995.
18. Moriyama K and Yahara I: Human CAP1 is a key factor in the recycling of cofilin and actin for rapid actin turnover. J Cell Sci 115: 1591-1601, 2002.
19. Hubberstey AV and Mottillo EP: Cyclase-associated proteins: CAPacity for linking signal transduction and actin polymerization. FASEB J 16: 487-499, 2002.
20. Loisel TP, Boujemaa R, Pantaloni D and Carlier MF: Reconstitution of actin-based motility of *Listeria* and *Shigella* using pure proteins. Nature 401: 613-616, 1999.
21. Yamazaki K, Takamura M, Masugi Y, *et al*: Adenylate cyclase-associated protein 1 overexpressed in pancreatic cancers is involved in cancer cell motility. Lab Invest 89: 425-432, 2009.